

ES-ENAS: BLACKBOX OPTIMIZATION OVER HYBRID SPACES VIA COMBINATORIAL AND CONTINUOUS EVOLUTION

Xingyou Song^{*1}, Krzysztof Choromanski^{1,2}, Jack Parker-Holder³, Yunhao Tang²,
 Daiyi Peng¹, Deepali Jain¹, Wenbo Gao⁴, Aldo Pacchiano⁵, Tamas Sarlos¹, Yuxiang Yang⁶
¹Google, ²Columbia University, ³Oxford University, ⁴Waymo, ⁵UC Berkeley,
⁶University of Washington

ABSTRACT

We consider the problem of efficient blackbox optimization over a large hybrid search space, consisting of a mixture of a high dimensional continuous space and a complex combinatorial space. Such examples arise commonly in evolutionary computation, but also more recently, neuroevolution and architecture search for Reinforcement Learning (RL) policies. In this paper, we introduce ES-ENAS, a simple joint optimization procedure by combining Evolutionary Strategies (ES) and combinatorial optimization techniques in a highly scalable and intuitive way, inspired by the *one-shot* or *supernet* paradigm introduced in Efficient Neural Architecture Search (ENAS). Our main insight is noticing that ES is already a highly distributed algorithm involving hundreds of blackbox evaluations which can not only be used for training neural network weights, but also for feedback to a combinatorial optimizer. Through this relatively simple marriage between two different lines of research, we are able to gain the best of both worlds, and empirically demonstrate our approach by optimizing BBOB functions over hybrid spaces as well as combinatorial neural network architectures via edge pruning and quantization on popular RL benchmarks. Due to the modularity of the algorithm, we also are able incorporate a wide variety of popular techniques ranging from use of different continuous and combinatorial optimizers, as well as constrained optimization.

1 INTRODUCTION AND RELATED WORK

We consider the problem of optimizing an expensive function $f : (\mathcal{M}, \mathbb{R}^d) \rightarrow \mathbb{R}$, where \mathcal{M} is a combinatorial search space consisting of potentially multiple layers of categorical and discrete variables, and \mathbb{R}^d is a high dimensional continuous search space, consisting of potentially hundreds to thousands of parameters. Such scenarios exist in reinforcement learning (RL), where $m \in \mathcal{M}$ represents an architecture specification and $\theta \in \mathbb{R}^d$ represents neural network weights, together to form a policy $\pi_{m,\theta} : \mathcal{S} \rightarrow \mathcal{A}$ in which the goal is to maximize total reward in a given environment. Other examples include flight optimization (Ahmad & Thomas, 2013), protein and chemical design (Elton et al., 2019; Zhou et al., 2017; Yang et al., 2019), and program synthesis (Summers, 1977).

There have been a flurry of previous methods for approaching complex, combinatorial search spaces, especially in the evolutionary algorithm domain, including the well-known NEAT (Stanley & Miikkulainen, 2002). Coincidentally, the neural architecture search (NAS) community has also adopted a multitude of blackbox optimization methods for dealing with NAS search spaces, including policy gradients via Pointer Networks (Vinyals et al., 2015) and more recently Regularized Evolution (Real et al., 2018). Such methods have been successfully applied to applications ranging from image classification (Zoph & Le, 2017) to language modeling (So et al., 2019), and even algorithm search/genetic programming (Real et al., 2020; Co-Reyes et al., 2021). Combinatorial algorithms allow huge flexibility in the search space definition, which allows optimization over generic spaces such as graphs, but many techniques rely on the notion of zeroth-order *mutation*, which can be

^{*}Correspondence to xingyousong@google.com.

Code: github.com/google-research/google-research/tree/master/es_enas

inappropriate in high dimensional continuous space due to large sample complexity (Nesterov & Spokoiny, 2017).

On the other hand, there are also a completely separate set of algorithms for attacking high dimensional continuous spaces \mathbb{R}^d . These include global optimization techniques including the Cross-Entropy method (de Boer et al., 2005) and metaheuristic methods such as swarm algorithms (Mavrouniotis et al., 2017). More local-search based techniques include the class of methods based on Evolution Strategies (ES) (Salimans et al., 2017), such as CMA-ES (Hansen et al., 2003; Krause et al., 2016; Varelak et al., 2018) and Augmented Random Search (ARS) (Mania et al., 2018b). ES has been shown to perform well for reinforcement learning policy optimization, especially in continuous control (Salimans et al., 2017) and robotics (Gao et al., 2020; Song et al., 2020a). Even though such methods are also zeroth-order, they have been shown to scale better than previously believed (Conti et al., 2018; Liu et al., 2019a; Rowland et al., 2018) on even millions of parameters (Such et al., 2017) due to advancements in heuristics (Choromanski et al., 2019a) and Monte Carlo gradient estimation techniques (Choromanski et al., 2019b; Yu et al., 2016). Unfortunately, these analytical techniques are limited only to continuous spaces and at best, basic categorical spaces via softmax reparameterization.

One may thus wonder whether it is possible to combine the two paradigms in an **efficient** manner. For example, in NAS applications, it would be extremely wasteful to run an end-to-end ES-based training loop for every architecture proposed by the combinatorial algorithm. At the same time, two practical design choices we must strive towards are also **simplicity** and **modularity**, in which a user may easily setup our method and arbitrarily swap in continuous algorithms like CMA-ES (Hansen et al., 2003) or combinatorial algorithms like Policy Gradients (Vinyals et al., 2015) and Regularized Evolution (Real et al., 2018), for specific scenarios. **Generality** is also an important aspect as well, in which our method should be applicable to generic hybrid spaces. For instance, HyperNEAT (Stanley et al., 2009) addresses the issue of high dimensional neural network weights by applying NEAT to evolve a smaller hypernetwork (Ha et al., 2017) for weight generation, but such a solution is domain specific and is not a general blackbox optimizer. Similarly restrictive, Weight Agnostic Neural Networks (Gaier & Ha, 2019) do not train any continuous parameters and applies NEAT to only the combinatorial space of network structures.

We are thus inspired by the joint optimization method from Efficient NAS (ENAS) (Pham et al., 2018), which introduces the notion of *weight sharing* to build a maximal *supernet* containing all possible weights θ_s where each *child model* m only utilizes certain subcomponents and their corresponding weights from this supernet. Child models m are sampled from a *controller* p_ϕ , parameterized by some state ϕ . **The core idea is to perform separate updates to θ_s and ϕ** in order to respectively, improve both neural network weights and architecture selection at the same time. However, ENAS was originally proposed in the setting of using a GPU worker with autodifferentiation over θ in mind for efficient NAS training.

In order to adopt ENAS’s joint optimization into the fully blackbox (and potentially non-differentiable) scenario involving hundreds/thousands of CPU-only workers, our key observation is that algorithms for combinatorial and continuous spaces commonly use very similar distributed workflows, involving usually a central *aggregator* and multiple parallel workers for function evaluations. Thus we may modify the aggregator to suggest a joint tuple (m, θ) , with function evaluations $f(m, \theta)$ used by both the combinatorial and continuous algorithms for improvement. A visual representation of our algorithm can be found in Fig. 1.

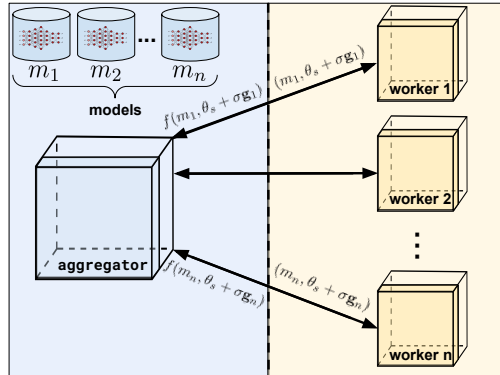


Figure 1: Figure representing our aggregator-worker pipeline when using a NAS controller with the vanilla ES method, where the aggregator proposes models m_i in addition to a perturbed input $\theta_s + \sigma_{g_i}$, and the worker the computes the objective $f(m_i, \theta_s + \sigma_{g_i})$, which is sent back to the aggregator. Both the training of the weights θ_s and of the model-proposing controller p_ϕ rely on the number of worker samples to improve performance.

We thus introduce the ES-ENAS algorithm, which is theoretically grounded, requires no extra computational resources, and is empirically effective on large hybrid search spaces ranging from categorized BBOB functions and neural network topologies.

2 ES-ENAS METHOD

2.1 PRELIMINARIES

We first define notation. Let \mathcal{M} be a combinatorial search space in which m are drawn from, and $\theta \in \mathbb{R}^d$ to be the continuous parameter. For scenarios such as NAS, one may define \mathcal{M} 's representation to be the superset of all possible child models m . Let ϕ represent the state of our combinatorial algorithm. Assuming this algorithm allows randomization, let p_ϕ be the current distribution over \mathcal{M} , where ϕ is to be optimized, and thus we may also sample $m \sim p_\phi$. We interchangeably refer to p_ϕ as also a ‘‘controller’’ using NAS terminology.

2.2 ALGORITHM

We concisely summarize our ES-ENAS method in Algorithm 1. For the sake of clarity, we use vanilla ES as the continuous optimizer and its derivation, but this can readily be changed to e.g. CMA-ES via replacing I with a learnable covariance matrix C for the perturbation $\mathbf{g} \sim \mathcal{N}(0, I)$ in Eq. 1, along with the update rule. Other ES variants (Wierstra et al., 2014; Heidrich-Meisner & Igel, 2009; Krause, 2019) can be swapped in similarly, although vanilla ES suffices for common problems such as continuous control. Below, we provide ES-ENAS’s derivation and conceptual simplicity of combining the updates for ϕ and θ into a joint optimization procedure.

The optimization problem we are interested in is $\max_{m \in \mathcal{M}, \theta \in \mathbb{R}^d} f(m, \theta)$. In order to make this problem tractable, consider instead, optimization on the smoothed objective:

$$\tilde{f}_\sigma(\phi, \theta) = \mathbb{E}_{m \sim p_\phi, \mathbf{g} \sim \mathcal{N}(0, I)} [f(m, \theta + \sigma \mathbf{g})] \quad (1)$$

The core trick is to use samples from $m \sim p_\phi, \mathbf{g} \sim \mathcal{N}(0, I)$ for updating both algorithm components in an unbiased manner.

2.2.1 UPDATING THE WEIGHTS

The gradient with respect to θ becomes:

$$\nabla_\theta \tilde{f}_\sigma(\phi, \theta) = \frac{1}{2\sigma} \mathbb{E}_{m \sim p_\phi, \mathbf{g} \sim \mathcal{N}(0, I)} [(f(m, \theta + \sigma \mathbf{g}) - f(m, \theta - \sigma \mathbf{g})) \mathbf{g}] \quad (2)$$

Note that by linearity, we may move the expectation $\mathbb{E}_{m \sim p_\phi}$ inside into the two terms $f(m, \theta + \sigma \mathbf{g})$ and $f(m, \theta - \sigma \mathbf{g})$, which implies that the gradient expression can be estimated with averaging singleton samples of the form:

$$\frac{1}{2\sigma} (f(m^+, \theta + \sigma \mathbf{g}) - f(m^-, \theta - \sigma \mathbf{g})) \mathbf{g} \quad (3)$$

where m^+, m^- are i.i.d. samples from p_ϕ , and \mathbf{g} from $\mathcal{N}(0, I)$.

Thus we may sample multiple i.i.d. child models $m_1^+, m_1^-, \dots, m_n^+, m_n^- \sim p_\phi$ and also multiple perturbations $\mathbf{g}_1, \dots, \mathbf{g}_n \sim \mathcal{N}(0, I)$ and update the shared weights θ_s with an approximate gradient

Algorithm 1: Default ES-ENAS Algorithm, with the few additional modifications to allow ENAS from ES shown in blue.

Data: Initial weights θ_s , weight step size η_w , precision parameter σ , number of perturbations n , controller p_ϕ .

```

while not done do
  Sample i.i.d. vectors
   $\mathbf{g}_1, \dots, \mathbf{g}_n \sim \mathcal{N}(0, \mathbf{I});$ 
  foreach  $\mathbf{g}_i$  do
    Sample  $m_i^+, m_i^- \sim p_\phi$ 
     $v_i^+ \leftarrow f(m_i^+, \theta_s + \sigma \mathbf{g}_i)$ 
     $v_i^- \leftarrow f(m_i^-, \theta_s - \sigma \mathbf{g}_i)$ 
     $v_i \leftarrow \frac{1}{2}(v_i^+ - v_i^-)$ 
     $p_\phi \leftarrow \{(m_i^+, v_i^+), (m_i^-, v_i^-)\}$ 
  end
  Update weights
   $\theta_s \leftarrow \theta_s + \eta_w \frac{1}{\sigma^n} \sum_{i=1}^n v_i \mathbf{g}_i$ 
  Update controller  $p_\phi$ 
end

```

end

update:

$$\theta_s \leftarrow \theta_s + \eta_w \left(\frac{1}{n} \sum_{i=1}^n \frac{f(m_i^+, \theta + \sigma \mathbf{g}_i) - f(m_i^-, \theta - \sigma \mathbf{g}_i)}{2\sigma} \mathbf{g}_i \right) \quad (4)$$

This update forms the ‘‘ES’’ portion of ES-ENAS. As a sanity check, we can see that using a constant fixed model $m = m_1^+ = m_1^- = \dots = m_n^+ = m_n^-$ reduces Eq. 4 to standard ES/ARS optimization.

2.2.2 UPDATING THE CONTROLLER

For the ‘‘ENAS’’ portion of ES-ENAS (i.e. for optimizing the $m \in \mathcal{M}$ component), we update p_ϕ by simply reusing the objectives $f(m, \theta + \sigma \mathbf{g})$ already computed for the weight updates, as they can be viewed as unbiased estimations of $\mathbb{E}_{\mathbf{g} \sim \mathcal{N}(0, I)}[f(m, \theta + \sigma \mathbf{g})]$ for a given m . Many methods can be classified within the following approaches:

Policy Gradient Methods: The ϕ are differentiable parameters of a distribution p_ϕ (usually a RNN-based controller), with the goal of optimizing the smoothed objective $J(\phi) = \mathbb{E}_{m \sim p_\phi, \mathbf{g} \sim \mathcal{N}(0, I)}[f(m; \theta_s + \mathbf{g})]$, whose *policy gradient* $\nabla_\phi J(\phi)$ can be estimated by:

$$\widehat{\nabla}_\phi J(\phi) = \frac{1}{n} \sum_{i=1}^n f(m_i, \theta_s + \mathbf{g}_i) \nabla_\phi \log p_\phi(m_i) \quad (5)$$

where $\log p_\phi(m)$ is the log-probability of the controller for selecting m , and thus $\phi \leftarrow \phi + \eta_{pg} \widehat{\nabla}_\phi J(\phi)$ is updated with the use of the REINFORCE algorithm (Williams, 1992), or other variants such as PPO (Schulman et al., 2017) and TRPO (Schulman et al., 2015). When combined with ES, a ‘‘simultaneous gradient’’ $\nabla_{\phi, \theta} \tilde{f}_\sigma(\phi, \theta)$ is thus effectively being estimated in ES-ENAS.

Evolutionary Algorithms: In this setting, ϕ represents the algorithm state, which usually consists of a *population* of inputs $Q = \{(m_1, \theta_1), \dots, (m_n, \theta_n)\}$ with corresponding evaluations (slightly abusing notation) $f(Q) = \{f(m_1, \theta_1), \dots, f(m_n, \theta_n)\}$. The algorithm performs a *selection procedure* which selects an individual (m_i, θ_i) or potentially multiple individuals $T \subseteq Q$, in order to perform respectively, mutation or crossover to ‘‘reproduce’’ and form a new child instance (m_{new}, θ_{new}) . Some prominent examples include Regularized Evolution (Real et al., 2018), NEAT (Stanley & Miikkulainen, 2002), and Hill-Climbing (Golovin et al., 2020; Song et al., 2020c).

2.3 CONVERGENCE AND EXTENSIONS

This mechanism shows that updates to the controller p_ϕ and updates to the weights θ_s *both rely* on the samples $f(m, \theta + \sigma \mathbf{g})$. The number of workers n , now serves the two purposes: reducing the sample complexity of the controller p_ϕ , as well as the variance of the estimated ES gradient $\nabla_\theta \tilde{f}_\sigma$. ES usually uses many more workers (on the order of 10^2) than what is normal in SL (on the order of 10^0 to 10^1 of workers) which can be important for the controller p_ϕ ’s performance, as we will demonstrate in Subsection 3.3.2.

Note that we may also modify Algorithm 1 in an alternating fashion to only update either ϕ or θ_s at each iteration without smoothing the other, as in the case of the original ENAS paper. This allows better theoretical properties if each of the continuous and categorical algorithms guarantee improvement alone. However, the tradeoff is at the cost of 2x the iteration count, and since objectives are commonly nonconvex, alternating optimization may not be necessary. We also verify empirically in Section 3 that our default Algorithm 1 consistently achieves convergence.

The combinatorial/controller algorithm p_ϕ ’s objective can also be defined differently from the weights θ_s ’s objective. This is already subtly the case in NAS, where the controller’s objective is the *nondifferentiable validation accuracy* of the model, while the model weights are explicitly optimizing against the *differentiable cross-entropy training loss* of the model. More significant differences between the two objectives involve cases such as efficiency and runtime of the network, which have led to work in EfficientNets (Tan & Le, 2019) via constrained optimization. We show this scenario can also be applied for the ES-ENAS setting in Subsection 3.3.4.

3 EXPERIMENTS

3.1 CURSE OF CONTINUOUS DIMENSIONALITY

We begin our experimental section by demonstrating the degradation of vanilla combinatorial evolutionary algorithms over 18 different Black-Box Optimization Benchmarking (BBOB) functions (Hansen et al., 2009), when the continuous space grows in size. We define our hybrid search space as $(\mathcal{M}, \mathbb{R}^{d_{con}})$, where \mathcal{M} consists of equally spaced gridpoints in $\mathbb{R}^{d_{cat}}$, which are then considered unordered categories. Thus $m \in \mathcal{M} \subset \mathbb{R}^{d_{cat}}$, which means an input (m, θ) can be used for a native continuous function f originally operating on the input space $\mathbb{R}^{d_{cat}+d_{con}}$. For practical purposes, we bound all parameters inside an interval $[-B, B]$, and set the optimum value of f to be 0, with the argmax argument also located when all parameters are zero valued.

For baselines, our combinatorial evolutionary algorithms include Regularized Evolution (Real et al., 2018), NEAT (Stanley & Miikkulainen, 2002), Random Search, and Gradientless Descent/Batch Hill-Climbing (Golovin et al., 2020; Song et al., 2020c). We also include PPO (Schulman et al., 2017) as a policy gradient baseline, but only for categorical parameters as Pointer Networks do not support continuous parameters and ES can already be considered a policy gradient/smoothed gradient approach. In order to remain fair and consistent across all evolutionary algorithms (including ES), we use the same mutation for continuous parameters $\theta \in \mathbb{R}^{d_{con}}$, which consists of applying a random Gaussian perturbation $\theta + \sigma_{mut}\mathbf{g}$ with a reasonable and tuned scaling σ_{mut} , as well as applying a uniformly random chosen categorical parameter from the d_{cat} parameters to resample. All algorithms start at the same randomly sampled initial point. More details can be found in Appendix A.3 along with continuous optimizer comparisons (including CMA-ES) in Appendix B.

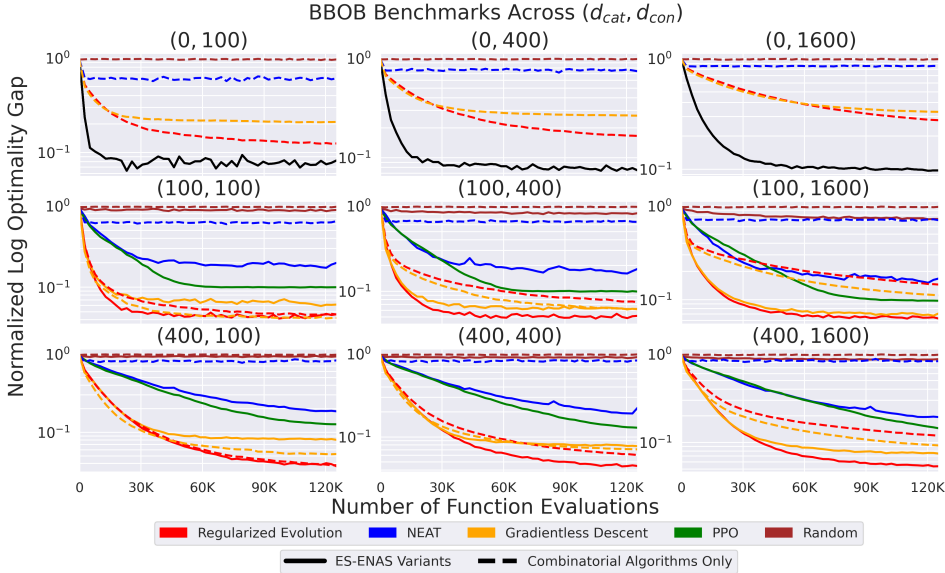


Figure 2: Plot of average normalized optimality gap across all BBOB functions (3 seeds each), when ranging d_{cat} and d_{con} . As d_{con} increases, over all combinatorial algorithms (different colors), each ES-ENAS variant (solid line) begins to outperform its corresponding vanilla combinatorial algorithm (dashed line). Note that if $d_{cat} = 0$, all ES-ENAS variants are equivalent to Vanilla ES (single black solid line, 1st row).

3.2 NEURAL NETWORK POLICIES

In order to benchmark our method over more nested combinatorial structures, we apply our method to two combinatorial problems, **Sparsification** and **Quantization**, on standard Mujoco (Todorov et al., 2012) environments from OpenAI Gym, which is well aligned with the use of ES. One benefit specifically with ES when reducing parameter count is naturally improving sample complexity, as speed of optimization is inversely related to the input dimension (Jamieson et al., 2012; Storn & Price, 1997; Agarwal et al., 2011).

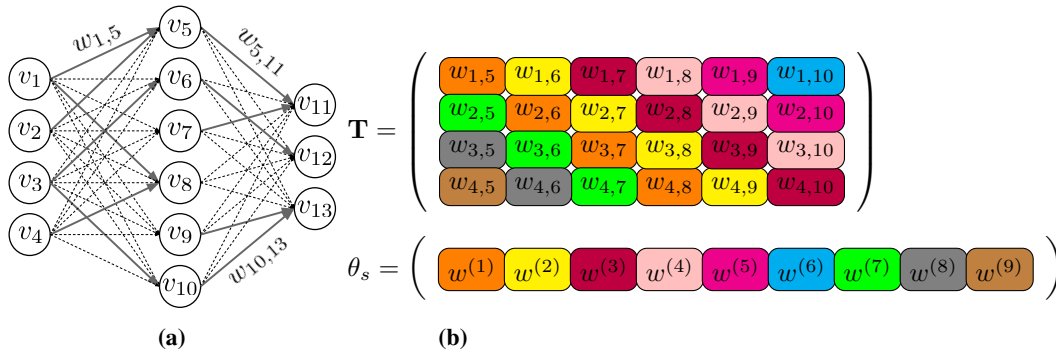


Figure 3: (a) Example of sparsifying a neural network setup, where solid edges are those learned by the algorithm. (b) Example of quantization using a Toeplitz pattern (Chromanski et al., 2018), for the first layer in Fig. 3a. Entries in each of the diagonals are colored the same, thus sharing the same weight value. The trainable weights $\theta_s = (w^{(1)}, \dots, w^{(9)})$ are denoted at the very bottom in the vectorized form with 9 entries, which effectively encodes the larger \mathbf{T} with 24 entries.

Such problems also have a long history, with sparsification methods such as (Rumelhart, 1987; Chauvin, 1989; Mozer & Smolensky, 1989) from the 1980’s, Optimal Brain Damage (Cun et al., 1990), regularization (Louizos et al., 2018), magnitude-based weight pruning methods (Han et al., 2015; See et al., 2016; Narang et al., 2017), sparse network learning (Gomez et al., 2019; Lenc et al., 2019), and the recent Lottery Ticket Hypothesis (Frankle & Carbin, 2019). Meanwhile, quantization has been explored with Huffman coding (Han et al., 2016), randomized quantization (Chen et al., 2015), and hashing mechanisms (Eban et al., 2020).

3.2.1 RESULTS

We can view a feedforward neural network as a standard directed acyclic graph (DAG), with a set of *vertices* containing values $\{v_1, \dots, v_k\}$, and a set of *edges* $\{(i, j) \mid 1 \leq i \leq j \leq k\}$ where each edge (i, j) contains a weight $w_{i,j}$, as shown in Figures 3a and 3b. The goal of sparsification is to reduce the number of edges while maintaining high environment reward, while the goal of quantization is to partition the edges via *colorings*, which allows same-colored edges to use the same weight. These scenarios possess very large combinatorial policy search spaces (calculated as $|\mathcal{M}| > 10^{68}$, comparable to 10^{49} from NASBench-101 (Ying et al., 2019)) that will stress test our ES-ENAS algorithm and are also relevant to mobile robotics (Gage, 2002). Given the results in Subsection 3.1 and since this is a NAS-based problem, for ES-ENAS we use the two most domain-specific controllers, Regularized Evolution and PPO (Policy Gradient) and take the best result in each scenario. Specific details and search space size calculations can be found in Appendix A.4.

As we have already demonstrated comparisons to blackbox optimization baselines in Subsection 3.1, we instead focus our comparison to domain-specific baselines for the neural network. These include a DARTS-like (Liu et al., 2019b) softmax *masking* method (Lenc et al., 2019), where a trainable boolean matrix mask is applied over the weights for edge pruning. We also include fixed quantization patterns such as Toeplitz and Circulant

Env.	Arch.	Reward	# weights	compression	# bits
Striker	Quantization	-247	23	95%	8198
	Edge Pruning	-130	64	93%	3072
	Masked	-967	25	95%	8262
	Toeplitz	-129	110	88%	4832
	Circulant	-120	82	90%	3936
	Unstructured	-117	1230	0%	40672
HalfCheetah	Quantization	4894	17	94%	6571
	Edge Pruning	4016	64	98%	3072
	Masked	4806	40	92%	8250
	Toeplitz	2525	103	85%	4608
	Circulant	1728	82	88%	3936
	Unstructured	3614	943	0%	31488
Hopper	Quantization	3220	11	92%	3960
	Edge Pruning	3349	64	84%	3072
	Masked	2196	17	91%	4726
	Toeplitz	2749	94	78%	4320
	Circulant	2680	82	80%	3936
	Unstructured	2691	574	0%	19680
Walker2d	Quantization	2026	17	94%	6571
	Edge Pruning	3813	64	90%	3072
	Masked	1781	19	94%	6635
	Toeplitz	1	103	85%	4608
	Circulant	3	82	88%	3936
	Unstructured	2230	943	0%	31488

Table 1: Comparison of the best policies from six distinct classes of RL networks: Quantization (ours), Edge Pruning (ours), Masked, Toeplitz, Circulant, and Unstructured networks trained with standard ES algorithm (Salimans et al., 2017). All results are for feedforward nets with one hidden layer. Best two metrics for each environment are in **bold**, while significantly low rewards are in **red**.

(particular class of Toeplitz) matrices, which are strong mathematically grounded baselines from (Choromanski et al., 2018). In all cases we use the same hyper-parameters, and train until convergence for three random seeds. For masking, we report the best achieved reward with $> 90\%$ of the network pruned, making the final policy comparable in size to the quantization and edge-pruning networks. Specific details can be found in Appendices C.1 and A.4.

For each class of policies, we compare various metrics, such as the number of weight parameters used, total parameter count compression with respect to unstructured networks, and total number of bits for encoding float values (since quantization and masking methods require extra bits to encode the partitioning via dictionaries).

As we can see in Table 1, both sparsification and quantization can be **learned from scratch via optimization using ES-ENAS**, which achieves competitive or better rewards against other baselines. This is especially true against hand-designed (Toeplitz/Circulant) patterns which significantly fail at Walker2d, as well as other optimization-based reparameterizations, such as softmax masking, which underperforms on the majority of environments.

The full set of numerical results over all of the mentioned methods can be found in Appendix C, which includes quantization (Appendix C.2), edge pruning and nonlinearity search (Appendix C.3), as well as plots for baseline methods (Fig. 9).

3.3 NEURAL NETWORK POLICY ABLATIONS

In the rest of the experimental section, we provide ablations studies on the properties and extensions of our ES-ENAS method. Because of the nested combinatorial structure of the neural network space (rather than the flat space of BBOB functions), many desired behaviors for the algorithm are no longer obvious nor visualizable at first sight. These behaviors include as raised questions, which also highlight certain similarities and differences from regular NAS in supervised learning:

1. How do controllers compare in performance?
2. How does the number of workers affect the quality of optimization?
3. Does the algorithm converge properly to a fixed architecture m ?
4. Does constrained optimization also work in ES-ENAS?

3.3.1 CONTROLLER COMPARISONS

As shown in Subsection 3.1, Regularized Evolution (Reg-Evo) was the highest performing controller when used in ES-ENAS. However, this is not always the case, as mutation-based optimization may be prone to being stuck in local optima whereas policy gradient methods (PG) such as PPO can allow better exploration.

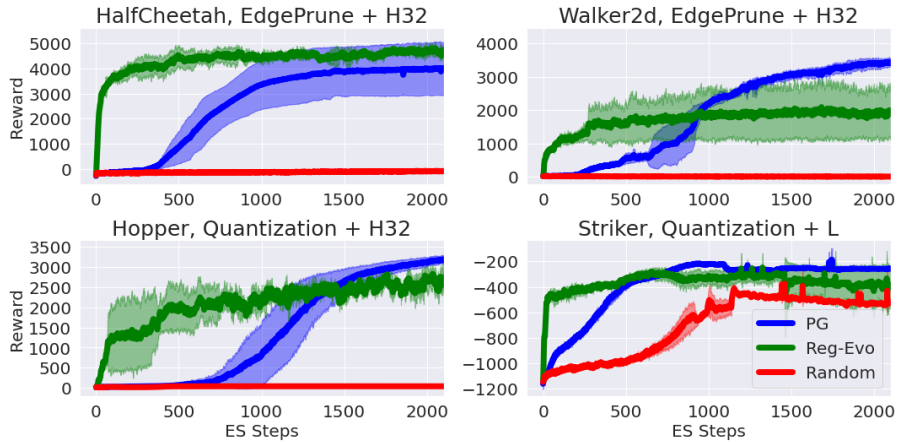


Figure 4: Comparisons across different environments when using different controllers, on the edge pruning and quantization tasks, when using a linear layer (L) or hidden layer of size 32 (H32).

We thus compare different ES-ENAS variants, when using Reg-Evo, PG (PPO), and random search (for sanity checking), on the edge pruning task in Fig. 4. As shown, while Reg-Evo consistently converges faster than PG at first, PG eventually may outperform Reg-Evo in asymptotic performance. Previously on NASBENCH-like benchmarks, Reg-Evo consistently outperforms PG in both sample complexity and asymptotic performance (Real et al., 2018), and thus our results on ES-ENAS are surprising, potentially due to the hybrid optimization of ES-ENAS.

Random search has been shown in supervised learning to be a surprisingly strong baseline (Li & Talwalkar, 2019), with the ability to produce even ≥ 80 -90 % accuracy (Pham et al., 2018; Real et al., 2018), showing that NAS-based optimization produces most gains ultimately be at the tail end; e.g. at the 95% accuracies. In the ES-ENAS setting, this is shown to occur for easier RL environments such as Striker (Fig. 4) and Reacher (shown in Appendices C.2, C.3). However, for the majority of RL environments, a random search controller is unable to train at all, which also makes this regime different from supervised learning.

3.3.2 CONTROLLER SAMPLE COMPLEXITY

We further investigate the effect of the number of objective values per batch on the controller by randomly selecting only a subset of the objectives $f(m, \theta)$ for the controller p_ϕ to use, but maintain the original number of workers for updating θ_s via ES to maintain weight estimation quality to prevent confounding results. We found that this sample reduction can reduce the performance of both controllers for various tasks, especially the PG controller. Thus, we find the **use of the already present ES workers highly crucial** for the controller’s quality of architecture search in this setting.

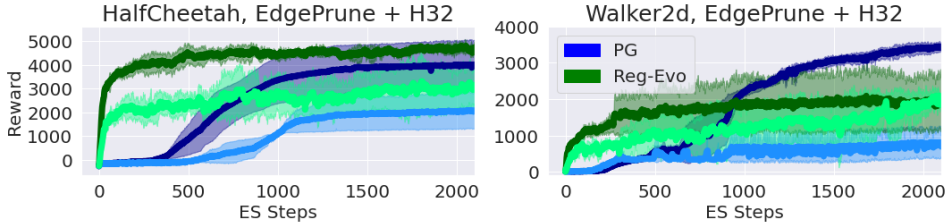


Figure 5: Regular ES-ENAS experiments with 150 full controller objective value usage plotted in darker colors. Experiments with lower controller sample usage (10 random samples, similar to the number of simultaneously training models in (Tan et al., 2018b)) plotted in corresponding lighter colors.

3.3.3 VISUALIZING AND VERIFYING CONVERGENCE

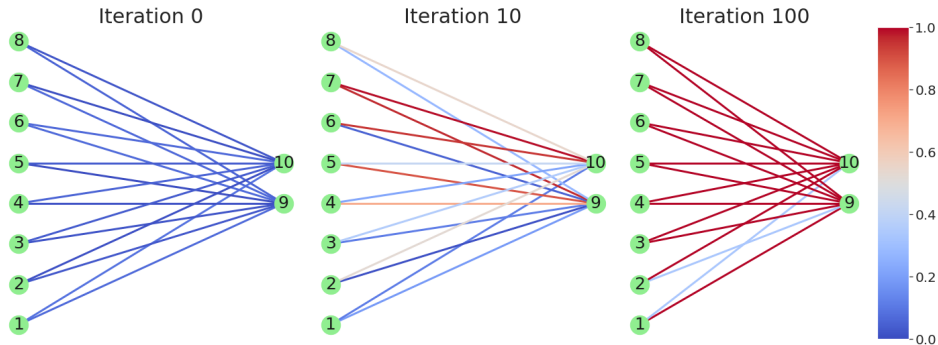


Figure 6: Edge pruning convergence over time, with samples aggregated over 3 seeds from PG runs on Swimmer. Each edge is colored according to a spectrum, with its color value equal to $2|p - \frac{1}{2}|$ where p is the edge frequency. We see that initially, each edge has uniform ($p = \frac{1}{2}$) probability of being selected, but as the controller trains, the samples converge toward a single pruning.

We also graphically plot aggregate statistics over the controller samples to confirm ES-ENAS’s convergence. We choose the smallest environment, Swimmer, which conveniently works particularly

well with *linear* policies (Mania et al., 2018b), to reduce visual complexity and avoid permutation invariances. We also use a boolean mask space over all possible edges (search space size $|\mathcal{M}| = 2^{|S| \times |A|} = 2^{8 \times 2}$). We remarkably observe that *for all 3 independently seeded runs*, PG converges toward a specific “local maximum” architecture, demonstrated in Fig. 6 with the final architecture presented in Appendix D, which also depicts a similar case for Reg-Evo. This suggests that there may be a few “natural architectures” optimal to the state representation.

3.3.4 CONSTRAINED OPTIMIZATION

(Tan & Le, 2019; Tan et al., 2018b) introduce the powerful notion of *constrained optimization*, where the controller may optimize multiple objectives (ex: efficiency) towards a Pareto optimal solution (Deb, 2005). We apply (Tan et al., 2018b) and modify the controller’s objective to be a hybrid combination $f(m, \theta) \left(\frac{|E_m|}{|E_T|} \right)^\omega$ of both the total reward $f(m, \theta)$ and the compression ratio $\frac{|E_m|}{|E_T|}$ where $|E_m|$ is the number of edges in model m and $|E_T|$ is a target number, with the search space expressed as boolean mask mappings $(i, j) \rightarrow \{0, 1\}$ over all possible edges. For simplicity, we use the naive setting in (Tan et al., 2018b) and set $\omega = -1$ if $\frac{|E_m|}{|E_T|} > 1$, while $\omega = 0$ otherwise, which strongly penalizes the controller if it proposes a model m whose edge number $|E_m|$ breaks the threshold $|E_T|$.

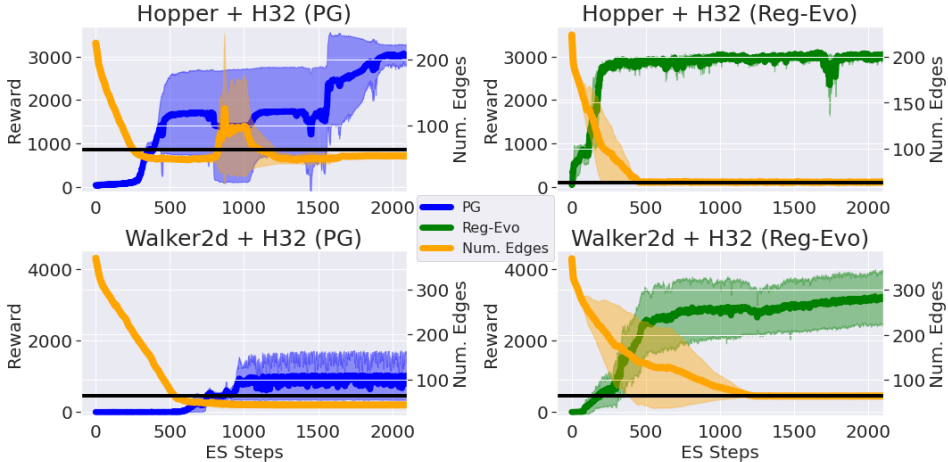


Figure 7: Environment reward plotted alongside the average number of edges used for proposed models. **Black horizontal line** corresponds to the target $|E_T| = 64$.

In Fig. 7, we see that the controller eventually reduces the number of edges below the target threshold set at $|E_T| = 64$, while still maintaining competitive training reward, demonstrating that ES-ENAS is also capable of constrained optimization techniques, potentially useful for explicitly designing efficient CPU-constrained robot policies (Unitree, 2017; Gao et al., 2020; Tan et al., 2018a).

4 CONCLUSION & FUTURE WORK

We presented a scalable and flexible algorithm, ES-ENAS, for performing combinatorial optimization over hybrid spaces and efficient architecture search for ES-trained neural networks such as reinforcement learning policies. ES-ENAS is efficient, simple, modular, and general-purpose, and can utilize many techniques from both the continuous and combinatorial evolutionary literature.

We believe that this work can be useful for several downstream applications, such as designing new architectures for mobile robotics, including compact cells for vision-based RL policies to improve generalization (Cobbe et al., 2020; 2019; Song et al., 2020b) and RNNs for meta-learning and memory (Bakker, 2001; Najarro & Risi, 2020). Outside of RL, our method contributes to the general blackbox optimization literature, such as hyperparameter tuning (Golovin et al., 2017), and may potentially be applicable to Bayesian Optimization for hybrid spaces (Deshwal et al., 2021).

5 ACKNOWLEDGEMENTS

The authors would like to thank David Ha, Esteban Real, Yingjie Miao, Qiuyi Zhang, Aleksandra Faust, Sagi Perel, Daniel Golovin, John D. Co-Reyes, and Vikas Sindhwani for valuable discussions.

REFERENCES

- Alekh Agarwal, Dean P. Foster, Daniel J. Hsu, Sham M. Kakade, and Alexander Rakhlin. Stochastic convex optimization with bandit feedback. In *Advances in Neural Information Processing Systems 24: 25th Annual Conference on Neural Information Processing Systems 2011. Proceedings of a meeting held 12-14 December 2011, Granada, Spain*, pp. 1035–1043, 2011. URL <http://papers.nips.cc/paper/4475-stochastic-convex-optimization-with-bandit-feedback>.
- Sohail Ahmad and K. Thomas. Flight optimization system (flops) hybrid electric aircraft design capability. 2013.
- Bram Bakker. Reinforcement learning with long short-term memory. In *Advances in Neural Information Processing Systems 14: Annual Conference on Neural Information Processing Systems 2001, NeurIPS 2001*, 2001.
- Yves Chauvin. A back-propagation algorithm with optimal use of hidden units. In David S. Touretzky (ed.), *Advances in Neural Information Processing Systems 1*, pp. 519–526, San Francisco, CA, USA, 1989. Morgan Kaufmann Publishers Inc.
- Wenlin Chen, James Wilson, Stephen Tyree, Kilian Weinberger, and Yixin Chen. Compressing neural networks with the hashing trick. In *International Conference on Machine Learning*, pp. 2285–2294, 2015.
- Krzysztof Choromanski, Mark Rowland, Vikas Sindhwani, Richard E. Turner, and Adrian Weller. Structured evolution with compact architectures for scalable policy optimization. In *Proceedings of the 35th International Conference on Machine Learning, ICML 2018, Stockholmsmässan, Stockholm, Sweden, July 10-15, 2018*, pp. 969–977, 2018.
- Krzysztof Choromanski, Aldo Pacchiano, Jack Parker-Holder, Yunhao Tang, Deepali Jain, Yuxiang Yang, Atil Iscen, Jasmine Hsu, and Vikas Sindhwani. Provably robust blackbox optimization for reinforcement learning. In *3rd Annual Conference on Robot Learning, CoRL 2019, Osaka, Japan, October 30 - November 1, 2019, Proceedings*, pp. 683–696, 2019a. URL <http://proceedings.mlr.press/v100/choromanski20a.html>.
- Krzysztof Choromanski, Aldo Pacchiano, Jack Parker-Holder, Yunhao Tang, and Vikas Sindhwani. From complexity to simplicity: Adaptive es-active subspaces for blackbox optimization. In *Advances in Neural Information Processing Systems 32: Annual Conference on Neural Information Processing Systems 2019, NeurIPS 2019, December 8-14, 2019, Vancouver, BC, Canada*, pp. 10299–10309, 2019b.
- John D. Co-Reyes, Yingjie Miao, Daiyi Peng, Esteban Real, Sergey Levine, Quoc V. Le, Honglak Lee, and Aleksandra Faust. Evolving reinforcement learning algorithms. *CoRR*, abs/2101.03958, 2021. URL <https://arxiv.org/abs/2101.03958>.
- Karl Cobbe, Oleg Klimov, Christopher Hesse, Taehoon Kim, and John Schulman. Quantifying generalization in reinforcement learning. In *Proceedings of the 36th International Conference on Machine Learning, ICML 2019, 9-15 June 2019, Long Beach, California, USA*, pp. 1282–1289, 2019. URL <http://proceedings.mlr.press/v97/cobbe19a.html>.
- Karl Cobbe, Christopher Hesse, Jacob Hilton, and John Schulman. Leveraging procedural generation to benchmark reinforcement learning. In *Proceedings of the 37th International Conference on Machine Learning, ICML 2020, 13-18 July 2020, Virtual Event*, pp. 2048–2056, 2020. URL <http://proceedings.mlr.press/v119/cobbe20a.html>.

- Edoardo Conti, Vashisht Madhavan, Felipe Petroski Such, Joel Lehman, Kenneth O. Stanley, and Jeff Clune. Improving exploration in evolution strategies for deep reinforcement learning via a population of novelty-seeking agents. In Samy Bengio, Hanna M. Wallach, Hugo Larochelle, Kristen Grauman, Nicolò Cesa-Bianchi, and Roman Garnett (eds.), *Advances in Neural Information Processing Systems 31: Annual Conference on Neural Information Processing Systems 2018, NeurIPS 2018, December 3-8, 2018, Montréal, Canada*, pp. 5032–5043, 2018. URL <https://proceedings.neurips.cc/paper/2018/hash/b1301141feffabac455e1f90a7de2054-Abstract.html>.
- Yann Le Cun, John S. Denker, and Sara A. Solla. Optimal brain damage. In David S. Touretzky (ed.), *Advances in Neural Information Processing Systems 2*, San Francisco, CA, USA, 1990. Morgan Kaufmann Publishers Inc.
- Pieter-Tjerk de Boer, Dirk P. Kroese, Shie Mannor, and Reuven Y. Rubinstein. A tutorial on the cross-entropy method. *Ann. Oper. Res.*, 134(1):19–67, 2005. doi: 10.1007/s10479-005-5724-z. URL <https://doi.org/10.1007/s10479-005-5724-z>.
- Kalyanmoy Deb. *Multi-Objective Optimization*. Springer US, 2005. ISBN 978-0-387-28356-2. doi: 10.1007/0-387-28356-0.10.
- Aryan Deshwal, Syrine Belakaria, and Janardhan Rao Doppa. Bayesian optimization over hybrid spaces. In Marina Meila and Tong Zhang (eds.), *Proceedings of the 38th International Conference on Machine Learning, ICML 2021, 18-24 July 2021, Virtual Event*, volume 139 of *Proceedings of Machine Learning Research*, pp. 2632–2643. PMLR, 2021. URL <http://proceedings.mlr.press/v139/deshwal21a.html>.
- Elad Eban, Yair Movshovitz-Attias, Hao Wu, Mark Sandler, Andrew Poon, Yerlan Idelbayev, and Miguel Á. Carreira-Perpiñán. Structured multi-hashing for model compression. In *2020 IEEE/CVF Conference on Computer Vision and Pattern Recognition, CVPR 2020, Seattle, WA, USA, June 13-19, 2020*, pp. 11900–11909, 2020. doi: 10.1109/CVPR42600.2020.01192.
- Daniel C. Elton, Zois Boukouvalas, Mark D. Fuge, and Peter W. Chung. Deep learning for molecular generation and optimization - a review of the state of the art. *CoRR*, abs/1903.04388, 2019. URL <http://arxiv.org/abs/1903.04388>.
- Jonathan Frankle and Michael Carbin. The lottery ticket hypothesis: Finding sparse, trainable neural networks. In *7th International Conference on Learning Representations, ICLR 2019, New Orleans, LA, USA, May 6-9, 2019*. OpenReview.net, 2019. URL <https://openreview.net/forum?id=rJl-b3RcF7>.
- Douglas W. Gage (ed.). *Mobile Robots XVII, Philadelphia, PA, USA, October 25, 2004*, volume 5609 of *SPIE Proceedings*, 2002. SPIE. ISBN 978-0-8194-5562-8. URL <http://proceedings.spiedigitallibrary.org/volume.aspx?volume=5609>.
- Adam Gaier and David Ha. Weight agnostic neural networks. In *Advances in Neural Information Processing Systems 32: Annual Conference on Neural Information Processing Systems 2019, NeurIPS 2019, December 8-14, 2019, Vancouver, BC, Canada*, pp. 5365–5379, 2019. URL <http://papers.nips.cc/paper/8777-weight-agnostic-neural-networks>.
- Wenbo Gao, Laura Graesser, Krzysztof Choromanski, Xingyou Song, Nevena Lazic, Pannag Sanketi, Vikas Sindhwani, and Navdeep Jaitly. Robotic table tennis with model-free reinforcement learning. 2020. URL <https://arxiv.org/abs/2003.14398>.
- Daniel Golovin, Benjamin Solnik, Subhodeep Moitra, Greg Kochanski, John Karro, and D. Sculley. Google vizier: A service for black-box optimization. In *Proceedings of the 23rd ACM SIGKDD International Conference on Knowledge Discovery and Data Mining, Halifax, NS, Canada, August 13 - 17, 2017*, pp. 1487–1495, 2017. doi: 10.1145/3097983.3098043.
- Daniel Golovin, John Karro, Greg Kochanski, Chansoo Lee, Xingyou Song, and Qiuyi Zhang. Gradientless descent: High-dimensional zeroth-order optimization. In *8th International Conference on Learning Representations, ICLR 2020, Addis Ababa, Ethiopia, April 26-30, 2020*. OpenReview.net, 2020. URL <https://openreview.net/forum?id=Skep6TVYDB>.

- Aidan N. Gomez, Ivan Zhang, Kevin Swersky, Yarín Gal, and Geoffrey E. Hinton. Learning sparse networks using targeted dropout. *ArXiv*, abs/1905.13678, 2019.
- David Ha, Andrew M. Dai, and Quoc V. Le. Hypernetworks. In *5th International Conference on Learning Representations, ICLR 2017, Toulon, France, April 24-26, 2017, Conference Track Proceedings*. OpenReview.net, 2017. URL <https://openreview.net/forum?id=rkpACellx>.
- Song Han, Jeff Pool, John Tran, and William Dally. Learning both weights and connections for efficient neural network. In C. Cortes, N. D. Lawrence, D. D. Lee, M. Sugiyama, and R. Garnett (eds.), *Advances in Neural Information Processing Systems 28*, pp. 1135–1143. Curran Associates, Inc., 2015.
- Song Han, Huizi Mao, and William J. Dally. Deep compression: Compressing deep neural network with pruning, trained quantization and Huffman coding. In *International Conference on Learning Representations*, 2016.
- Nikolaus Hansen, Sibylle D. Müller, and Petros Koumoutsakos. Reducing the time complexity of the derandomized evolution strategy with covariance matrix adaptation (cma-es). *Evol. Comput.*, 11(1):1–18, March 2003.
- Nikolaus Hansen, Steffen Finck, Raymond Ros, and Anne Auger. Real-Parameter Black-Box Optimization Benchmarking 2009: Noiseless Functions Definitions. Research Report RR-6829, INRIA, 2009. URL <https://hal.inria.fr/inria-00362633>.
- Verena Heidrich-Meisner and Christian Igel. Neuroevolution strategies for episodic reinforcement learning. *J. Algorithms*, 64(4):152–168, 2009. doi: 10.1016/j.jalgor.2009.04.002. URL <https://doi.org/10.1016/j.jalgor.2009.04.002>.
- Kevin G. Jamieson, Robert D. Nowak, and Benjamin Recht. Query complexity of derivative-free optimization. In *Advances in Neural Information Processing Systems 25: 26th Annual Conference on Neural Information Processing Systems 2012. Proceedings of a meeting held December 3-6, 2012, Lake Tahoe, Nevada, United States*, pp. 2681–2689, 2012. URL <http://papers.nips.cc/paper/4509-query-complexity-of-derivative-free-optimization>.
- Oswin Krause. Large-scale noise-resilient evolution-strategies. In *Proceedings of the Genetic and Evolutionary Computation Conference, GECCO '19*, pp. 682–690, New York, NY, USA, 2019. Association for Computing Machinery. ISBN 9781450361118. doi: 10.1145/3321707.3321724. URL <https://doi.org/10.1145/3321707.3321724>.
- Oswin Krause, Dídac Rodríguez Arbonès, and Christian Igel. CMA-ES with optimal covariance update and storage complexity. In Daniel D. Lee, Masashi Sugiyama, Ulrike von Luxburg, Isabelle Guyon, and Roman Garnett (eds.), *Advances in Neural Information Processing Systems 29: Annual Conference on Neural Information Processing Systems 2016, December 5-10, 2016, Barcelona, Spain*, pp. 370–378, 2016. URL <https://proceedings.neurips.cc/paper/2016/hash/289dff07669d7a23de0ef88d2f7129e7-Abstract.html>.
- Karel Lenc, Erich Elsen, Tom Schaul, and Karen Simonyan. Non-differentiable supervised learning with evolution strategies and hybrid methods. *arXiv*, abs/1906.03139, 2019.
- Liam Li and Ameet Talwalkar. Random search and reproducibility for neural architecture search. In Amir Globerson and Ricardo Silva (eds.), *Proceedings of the Thirty-Fifth Conference on Uncertainty in Artificial Intelligence, UAI 2019, Tel Aviv, Israel, July 22-25, 2019*, volume 115 of *Proceedings of Machine Learning Research*, pp. 367–377. AUAI Press, 2019.
- Guoqing Liu, Li Zhao, Feidiao Yang, Jiang Bian, Tao Qin, Nenghai Yu, and Tie-Yan Liu. Trust region evolution strategies. In *The Thirty-Third AAAI Conference on Artificial Intelligence, AAAI 2019, The Thirty-First Innovative Applications of Artificial Intelligence Conference, IAAI 2019, The Ninth AAAI Symposium on Educational Advances in Artificial Intelligence, EAAI 2019, Honolulu, Hawaii, USA, January 27 - February 1, 2019*, pp. 4352–4359. AAAI Press, 2019a. doi: 10.1609/aaai.v33i01.33014352. URL <https://doi.org/10.1609/aaai.v33i01.33014352>.

- Hanxiao Liu, Karen Simonyan, and Yiming Yang. DARTS: differentiable architecture search. In *7th International Conference on Learning Representations, ICLR 2019, New Orleans, LA, USA, May 6-9, 2019*, 2019b. URL <https://openreview.net/forum?id=S1eYHoC5FX>.
- Christos Louizos, Max Welling, and Diederik P. Kingma. Learning sparse neural networks through l0 regularization. In *International Conference on Learning Representations*, 2018.
- Horia Mania, Aurelia Guy, and Benjamin Recht. Simple random search provides a competitive approach to reinforcement learning. *CoRR*, abs/1803.07055, 2018a.
- Horia Mania, Aurelia Guy, and Benjamin Recht. Simple random search of static linear policies is competitive for reinforcement learning. In *Advances in Neural Information Processing Systems*, pp. 1800–1809, 2018b.
- Michalis Mavrouniotis, Changhe Li, and Shengxiang Yang. A survey of swarm intelligence for dynamic optimization: Algorithms and applications. *Swarm Evol. Comput.*, 33:1–17, 2017. doi: 10.1016/j.swevo.2016.12.005. URL <https://doi.org/10.1016/j.swevo.2016.12.005>.
- Michael C. Mozer and Paul Smolensky. Skeletonization: A technique for trimming the fat from a network via relevance assessment. In David S. Touretzky (ed.), *Advances in Neural Information Processing Systems 1*, pp. 107–115, San Francisco, CA, USA, 1989. Morgan Kaufmann Publishers Inc.
- Elias Najarro and Sebastian Risi. Meta-learning through hebbian plasticity in random networks. In Hugo Larochelle, Marc’Aurelio Ranzato, Raia Hadsell, Maria-Florina Balcan, and Hsuan-Tien Lin (eds.), *Advances in Neural Information Processing Systems 33: Annual Conference on Neural Information Processing Systems 2020, NeurIPS 2020, December 6-12, 2020, virtual*, 2020. URL <https://proceedings.neurips.cc/paper/2020/hash/ee23e7ad9b473ad072d57aaa9b2a5222-Abstract.html>.
- Sharan Narang, Gregory Diamos, Shubho Sengupta, and Erich Elsen. Exploring sparsity in recurrent neural networks. In *International Conference on Learning Representations*, 2017.
- Yurii E. Nesterov and Vladimir G. Spokoiny. Random gradient-free minimization of convex functions. *Found. Comput. Math.*, 17(2):527–566, 2017. doi: 10.1007/s10208-015-9296-2. URL <https://doi.org/10.1007/s10208-015-9296-2>.
- Daiyi Peng, Xuanyi Dong, Esteban Real, Mingxing Tan, Yifeng Lu, Gabriel Bender, Hanxiao Liu, Adam Kraft, Chen Liang, and Quoc Le. Pyglove: Symbolic programming for automated machine learning. In *Advances in Neural Information Processing Systems 33: Annual Conference on Neural Information Processing Systems 2020, NeurIPS 2020, December 6-12, 2020, virtual*, 2020. URL <https://proceedings.neurips.cc/paper/2020/hash/012a91467f210472fab4e11359bbfef6-Abstract.html>.
- Hieu Pham, Melody Y. Guan, Barret Zoph, Quoc V. Le, and Jeff Dean. Efficient neural architecture search via parameter sharing. In *Proceedings of the 35th International Conference on Machine Learning, ICML 2018, Stockholmsmässan, Stockholm, Sweden, July 10-15, 2018*, pp. 4092–4101, 2018.
- Esteban Real, Alok Aggarwal, Yanping Huang, and Quoc V. Le. Regularized evolution for image classifier architecture search. *CoRR*, abs/1802.01548, 2018. URL <http://arxiv.org/abs/1802.01548>.
- Esteban Real, Chen Liang, David R. So, and Quoc V. Le. Automl-zero: Evolving machine learning algorithms from scratch. *CoRR*, abs/2003.03384, 2020. URL <https://arxiv.org/abs/2003.03384>.
- Mark Rowland, Krzysztof Choromanski, François Chalus, Aldo Pacchiano, Tamás Szepesvári, Richard E. Turner, and Adrian Weller. Geometrically coupled monte carlo sampling. In Samy Bengio, Hanna M. Wallach, Hugo Larochelle, Kristen Grauman, Nicolò Cesa-Bianchi, and Roman Garnett (eds.), *Advances in Neural Information Processing Systems 31: Annual Conference on Neural Information Processing Systems 2018, NeurIPS 2018, December 3-8, 2018*,

- Montréal, Canada*, pp. 195–205, 2018. URL <https://proceedings.neurips.cc/paper/2018/hash/b3e3e393c77e35a4a3f3cbd1e429b5dc-Abstract.html>.
- D. E Rumelhart. Personal communication. *Princeton*, 1987.
- Tim Salimans, Jonathan Ho, Xi Chen, Szymon Sidor, and Ilya Sutskever. Evolution strategies as a scalable alternative to reinforcement learning. *arXiv*, abs/1703.03864, 2017.
- John Schulman, Sergey Levine, Pieter Abbeel, Michael Jordan, and Philipp Moritz. Trust region policy optimization. In *International Conference on Machine Learning (ICML)*, 2015.
- John Schulman, Filip Wolski, Prafulla Dhariwal, Alec Radford, and Oleg Klimov. Proximal policy optimization algorithms. *arXiv preprint arXiv:1707.06347*, 2017.
- Abigail See, Minh-Thang Luong, and Christopher D. Manning. Compression of neural machine translation models via pruning. In *Proceedings of The 20th SIGNLL Conference on Computational Natural Language Learning*, Berlin, Germany, August 2016. Association for Computational Linguistics.
- David R. So, Quoc V. Le, and Chen Liang. The evolved transformer. In *Proceedings of the 36th International Conference on Machine Learning, ICML 2019, 9-15 June 2019, Long Beach, California, USA*, pp. 5877–5886, 2019. URL <http://proceedings.mlr.press/v97/so19a.html>.
- Xingyou Song, Wenbo Gao, Yuxiang Yang, Krzysztof Choromanski, Aldo Pacchiano, and Yunhao Tang. ES-MAML: simple hessian-free meta learning. In *8th International Conference on Learning Representations, ICLR 2020, Addis Ababa, Ethiopia, April 26-30, 2020*, 2020a. URL <https://openreview.net/forum?id=SlExA2NtDB>.
- Xingyou Song, Yiding Jiang, Stephen Tu, Yilun Du, and Behnam Neyshabur. Observational overfitting in reinforcement learning. In *8th International Conference on Learning Representations, ICLR 2020, Addis Ababa, Ethiopia, April 26-30, 2020*, 2020b. URL <https://openreview.net/forum?id=HJli2hNKDH>.
- Xingyou Song, Yuxiang Yang, Krzysztof Choromanski, Ken Caluwaerts, Wenbo Gao, Chelsea Finn, and Jie Tan. Rapidly adaptable legged robots via evolutionary meta-learning. In *IEEE/RSJ International Conference on Intelligent Robots and Systems, IROS 2020, Las Vegas, NV, USA, October 24, 2020 - January 24, 2021*, pp. 3769–3776. IEEE, 2020c. doi: 10.1109/IROS45743.2020.9341571. URL <https://doi.org/10.1109/IROS45743.2020.9341571>.
- Kenneth O. Stanley and Risto Miikkulainen. Evolving neural network through augmenting topologies. *Evolutionary Computation*, 10(2):99–127, 2002.
- Kenneth O. Stanley, David B. D’Ambrosio, and Jason Gauci. A hypercube-based encoding for evolving large-scale neural networks. *Artif. Life*, 15(2):185–212, 2009. doi: 10.1162/artl.2009.15.2.15202. URL <https://doi.org/10.1162/artl.2009.15.2.15202>.
- Rainer Storn and Kenneth V. Price. Differential evolution - A simple and efficient heuristic for global optimization over continuous spaces. *J. Glob. Optim.*, 11(4):341–359, 1997. doi: 10.1023/A:1008202821328. URL <https://doi.org/10.1023/A:1008202821328>.
- Felipe Petroski Such, Vashisht Madhavan, Edoardo Conti, Joel Lehman, Kenneth O. Stanley, and Jeff Clune. Deep neuroevolution: Genetic algorithms are a competitive alternative for training deep neural networks for reinforcement learning. *CoRR*, abs/1712.06567, 2017. URL <http://arxiv.org/abs/1712.06567>.
- Phillip D. Summers. A methodology for lisp program construction from examples. *J. ACM*, 24(1):161–175, January 1977. ISSN 0004-5411. doi: 10.1145/321992.322002. URL <https://doi.org/10.1145/321992.322002>.

- Jie Tan, Tingnan Zhang, Erwin Coumans, Atil Iscen, Yunfei Bai, Danijar Hafner, Steven Bohez, and Vincent Vanhoucke. Sim-to-real: Learning agile locomotion for quadruped robots. In Hadas Kress-Gazit, Siddhartha S. Srinivasa, Tom Howard, and Nikolay Atanasov (eds.), *Robotics: Science and Systems XIV, Carnegie Mellon University, Pittsburgh, Pennsylvania, USA, June 26-30, 2018*, 2018a. doi: 10.15607/RSS.2018.XIV.010. URL <http://www.roboticsproceedings.org/rss14/p10.html>.
- Mingxing Tan and Quoc V. Le. Efficientnet: Rethinking model scaling for convolutional neural networks. In *Proceedings of the 36th International Conference on Machine Learning, ICML 2019, 9-15 June 2019, Long Beach, California, USA*, pp. 6105–6114, 2019. URL <http://proceedings.mlr.press/v97/tan19a.html>.
- Mingxing Tan, Bo Chen, Ruoming Pang, Vijay Vasudevan, and Quoc V. Le. Mnasnet: Platform-aware neural architecture search for mobile. *CoRR*, abs/1807.11626, 2018b. URL <http://arxiv.org/abs/1807.11626>.
- Emanuel Todorov, Tom Erez, and Yuval Tassa. Mujoco: A physics engine for model-based control. In *2012 IEEE/RSJ International Conference on Intelligent Robots and Systems, IROS 2012, Vilamoura, Algarve, Portugal, October 7-12, 2012*, pp. 5026–5033, 2012. doi: 10.1109/IROS.2012.6386109. URL <https://doi.org/10.1109/IROS.2012.6386109>.
- Unitree. Laikago website, 2017. URL <http://www.unitree.cc/e/action/ShowInfo.php?classid=6&id=1#>.
- Konstantinos Varelas, Anne Auger, Dimo Brockhoff, Nikolaus Hansen, Ouassim Ait ElHara, Yann Semet, Rami Kassab, and Frédéric Barbaresco. A comparative study of large-scale variants of CMA-ES. In Anne Auger, Carlos M. Fonseca, Nuno Lourenço, Penousal Machado, Luís Paquete, and L. Darrell Whitley (eds.), *Parallel Problem Solving from Nature - PPSN XV - 15th International Conference, Coimbra, Portugal, September 8-12, 2018, Proceedings, Part I*, volume 11101 of *Lecture Notes in Computer Science*, pp. 3–15. Springer, 2018. doi: 10.1007/978-3-319-99253-2_1. URL https://doi.org/10.1007/978-3-319-99253-2_1.
- Oriol Vinyals, Meire Fortunato, and Navdeep Jaitly. Pointer networks. In *Advances in Neural Information Processing Systems 28: Annual Conference on Neural Information Processing Systems 2015, December 7-12, 2015, Montreal, Quebec, Canada*, pp. 2692–2700, 2015.
- Daan Wierstra, Tom Schaul, Tobias Glasmachers, Yi Sun, Jan Peters, and Jürgen Schmidhuber. Natural evolution strategies. *Journal of Machine Learning Research*, 15:949–980, 2014.
- Ronald J. Williams. Simple statistical gradient-following algorithms for connectionist reinforcement learning. *Machine Learning*, 8:229–256, 1992. doi: 10.1007/BF00992696.
- Kevin K. Yang, Zachary Wu, and Frances H. Arnold. Machine learning-guided directed evolution for protein engineering, 2019.
- Chris Ying, Aaron Klein, Eric Christiansen, Esteban Real, Kevin Murphy, and Frank Hutter. Nasbench-101: Towards reproducible neural architecture search. In *Proceedings of the 36th International Conference on Machine Learning, ICML 2019, 9-15 June 2019, Long Beach, California, USA*, pp. 7105–7114, 2019. URL <http://proceedings.mlr.press/v97/ying19a.html>.
- Felix X Yu, Ananda Theertha Suresh, Krzysztof M Choromanski, Daniel N Holtmann-Rice, and Sanjiv Kumar. Orthogonal random features. In *Advances in Neural Information Processing Systems (NIPS)*. 2016.
- Zhenpeng Zhou, Xiaocheng Li, and Richard N. Zare. Optimizing chemical reactions with deep reinforcement learning. *ACS Central Science*, 3(12):1337–1344, 2017. doi: 10.1021/acscentsci.7b00492. URL <https://doi.org/10.1021/acscentsci.7b00492>. PMID: 29296675.
- Barret Zoph and Quoc V. Le. Neural architecture search with reinforcement learning. In *5th International Conference on Learning Representations, ICLR 2017, Toulon, France, April 24-26, 2017, Conference Track Proceedings*, 2017.

APPENDIX

A IMPLEMENTATION DETAILS

A.1 API

We use the standardized NAS API PyGlove (Peng et al., 2020), where search spaces are usually constructed via combinations of *primitives* such as `“pyglove.oneof”` and `“pyglove.manyof”` operations, which respectively choose one item, or a combination of multiple objects from a container. These primitives can be combined in a nested conditional structure via `“pyglove.List”` or `“pyglove.Dict”`. The search space can then be sent to an algorithm, which proposes child model instances m programmatically represented via Python dictionaries and strings. These are sent over a distributed communication channel to a worker alongside the perturbation $\theta + \sigma \mathbf{g}$, and then materialized later by the worker into an actual object such as a neural network. Although the controller needs to output hundreds of model suggestions, it can be parallelized to run quickly by multithreading (for Reg-Evo) or by simply using a GPU (for policy gradient).

A.2 ALGORITHMS

A.2.1 COMBINATORIAL ALGORITHMS

Regularized Evolution: We set the tournament size to be \sqrt{n} where n is the number of workers/population size, as this works best as a guideline (Real et al., 2018).

NEAT: We use the original algorithm specification of NEAT (Stanley & Miikkulainen, 2002) without additional modifications. The compatibility distance function was implemented appropriately for DNAs (i.e. “genomes”) in PyGlove, and a gridsweep was used to find the best coefficients.

Gradientless Descent/Batch Hill-Climbing: We use the same mutator throughout the optimization process, similar to (Song et al., 2020c) to reduce algorithm complexity, as the step size annealing schedule found in (Golovin et al., 2020) is specific to convex objectives only.

Policy Gradient: We use a gradient update batch size of 64 to the Pointer Network, while using PPO as the policy gradient algorithm, with its default (recommended) hyperparameters from (Peng et al., 2020).

A.2.2 CONTINUOUS ALGORITHMS

ARS/ES: We always use reward normalization and state normalization (for RL benchmarks) from (Mania et al., 2018a). For BBOB functions, we use $\eta_w = 0.5$ while $\sigma = 0.5$, along with 64 Gaussian directions per batch in an ES iteration, with 8 used for evaluation. For RL benchmarks, we use $\eta_w = 0.01$ and $\sigma = 0.1$, along with 75 Gaussian directions, with 50 more used for evaluation.

CMA-ES: For BBOB functions, we use $\sigma = 0.5$ and $\eta_w = 0.5$, similar to ARS/ES.

A.3 BBOB BENCHMARKS

Our BBOB functions consisted of the 18 classical functions from (Hansen et al., 2009): {Sphere, Rastrigin, BuecheRastrigin, LinearSlope, AttractiveSector, StepEllipsoidal, Rosenbrock-Rotated, Discus, BentCigar, SharpRidge, DifferentPowers, Weierstrass, SchaffersF7, SchaffersF7IIIConditioned, GriewankRosenbrock, Schwefel, Katsuura, Lunacek.}

The each parameter in the raw continuous input space is bounded within $[-B, B]$ where $B = 5$. For discretization + categorization into a grid, we use a granularity of 1 between consecutive points, i.e. a categorical a parameter is allowed to select within $\{-B, -B + 1, \dots, 0, \dots, B - 1, B\}$. Note that each BBOB function is set to have its global optimum at the zero-point, and thus our hybrid spaces contain the global optimum.

Because each BBOB function may have a completely different scaling (e.g. for a fixed dimension, the average output for Sphere may be within the order of 10^2 but the average output for BentCigar may be within 10^{10}), we thus normalize the output of each function when reporting results. The normalized valuation of a BBOB function f is calculated by dividing the raw value by the maximum absolute value obtained by random search.

Since for the ES component we use a step size of $\eta_w = 0.5$ and precision parameter of $\sigma = 0.5$, we thus use for evolutionary mutations, a Gaussian perturbation scaling σ_{mut} of 0.07, which equalizes the average norms between the update directions on θ , which are: $\eta_w \nabla_{\theta} \tilde{f}_{\sigma}$ and $\sigma_{mut} \mathbf{g}$.

A.4 RL + NEURAL NETWORK SETTING

In order to allow combinatorial flexibility, our neural network consists of vertices/values $V = \{v_1, \dots, v_k\}$, where the initial block of $|\mathcal{S}|$ values $\{v_1, \dots, v_{|\mathcal{S}|}\}$ corresponds to the environment state, and the last block of $|\mathcal{A}|$ values $\{v_{k-|\mathcal{A}|+1}, \dots, v_k\}$ corresponds to the action output values. Directed edges $E \subseteq E_{max} = \{e_{i,j} = (i,j) \mid 1 \leq i < j \leq k, |\mathcal{S}| < j\}$ are constructed with corresponding weights $W = \{w_{i,j} \mid (i,j) \in E\}$, and nonlinearities $G = \{\sigma_{|\mathcal{S}|+1}, \dots, \sigma_k\}$ for the non-state vertices. Thus a forward propagation consists of for-looping in order $j \in \{|\mathcal{S}|+1, \dots, k\}$ and computing output values $v_j = \sigma_j \left(\sum_{(i,j) \in E} v_i w_{i,j} \right)$.

By default, unless specified, we use Tanh non-linearities with 32 units for each hidden layer.

Edge pruning: We group all possible edges (i,j) into a set in the neural network, and select a fixed number of edges from this set. We can also further search across potentially different nonlinearities, e.g. $f_i \in \{\tanh, \text{sigmoid}, \text{sin}, \dots\}$ similarly to Weight Agnostic Neural Networks (Gaier & Ha, 2019). In terms of API, this search space can be described as `pyglove.manyof($E_{max}, |E|$)` along with `pyglove.oneof(σ_i, \mathcal{G})`. The search space is of size $\binom{|E_{max}|}{|E|}$ or $2^{|E_{max}|}$ when using a fixed or variable size $|E|$ respectively.

We collect all possible edges from a normal neural network into a pool E_{max} and set $|E| = 64$ as the number of distinct choices, passed to the `pyglove.manyof`. Similar to quantization, this choice is based on the value $\max(|\mathcal{S}|, H)$ or $\max(|\mathcal{A}|, H)$, where $H = 32$ is the number of hidden units, which is linear in proportion to respectively, the maximum number of weights $|\mathcal{S}| \cdot H$ or $|\mathcal{A}| \cdot H$. Since a hidden layer neural network has two weight matrices due to the hidden layer connecting to both the state and actions, we thus have ideally a maximum of $32 + 32 = 64$ edges.

For nonlinearity search, we use the same functions found in (Gaier & Ha, 2019). These are: {Tanh, ReLU, Exp, Identity, Sin, Sigmoid, Absolute Value, Cosine, Square, Reciprocal, Step Function.}

Quantization: We assign to each edge (i,j) one color of many $colors\ c \in \mathcal{C} = \{1, \dots, |\mathcal{C}|\}$, denoting the partition group the edge is assigned to, which defines the value $w_{i,j} \leftarrow w^{(c)}$. This is shown pictorially in Figs. 3a and 3b. This can also programmatically be done by concatenating primitives `pyglove.oneof($e_{i,j}, \mathcal{C}$)` over all edges $e_{i,j} \in E_{max}$. The search space is of size $|\mathcal{C}|^{|E|}$.

The number of partitions (or “colors”) is set to $\max(|\mathcal{S}|, |\mathcal{A}|)$. This is both in order to ensure a linear number of trainable parameters compared to the quadratic number for unstructured networks, as well as allow sufficient parameterization to deal with the entire state/action values.

A.4.1 ENVIRONMENT

For all environments, we set the horizon $T = 1000$. We also use the reward without alive bonuses for weight training as commonly used (Mania et al., 2018b) to avoid local maximum behaviors (such as an agent simply standing still to collect a total of 1000 reward), but report the final score as the real reward with the alive bonus.

A.4.2 BASELINE DETAILS

We consider Unstructured, Toeplitz, Circulant and a masking mechanism (Choromanski et al., 2018; Lenc et al., 2019). We introduce their details below. Notice that all baseline networks share the same general (1-hidden layer, Tanh nonlinearity) architecture from A.4. This implies that we only have two weight matrices $W_1 \in \mathbb{R}^{|\mathcal{S}| \times h}$, $W_2 \in \mathbb{R}^{h \times |\mathcal{A}|}$ and two bias vectors $b_1 \in \mathbb{R}^h$, $b_2 \in \mathbb{R}^{|\mathcal{A}|}$, where $|\mathcal{S}|$, $|\mathcal{A}|$ are dimensions of state/action spaces. These networks differ in how they parameterize the weight matrices. We have:

Unstructured: A fully-connected layer with unstructured weight matrix $W \in \mathbb{R}^{a \times b}$ has a total of ab independent parameters.

Toeplitz: A toeplitz weight matrix $W \in \mathbb{R}^{a \times b}$ has a total of $a+b-1$ independent parameters. This architecture has been shown to be effective in generating good performance on benchmark tasks yet compressing parameters (Choromanski et al., 2018).

Circulant: A circulant weight matrix $W \in \mathbb{R}^{a \times b}$ is defined for square matrices $a = b$. We generalize this definition by considering a square matrix of size $n \times n$ where $n = \max\{a, b\}$ and then do a proper truncation. This produces n independent parameters.

Masking: One additional technique for reducing the number of independent parameters in a weight matrix is to mask out redundant parameters (Lenc et al., 2019). This slightly differs from the other aforementioned architectures since these other architectures allow for parameter sharing while the masking mechanism carries out pruning. To be concrete, we consider a fully-connected matrix $W \in \mathbb{R}^{a \times b}$ with ab independent parameters. We also setup another mask weight $\Gamma \in \mathbb{R}^{a \times b}$. Then the mask is generated via

$$\Gamma' = \text{softmax}(\Gamma/\alpha)$$

where softmax is applied elementwise and α is a constant. We set $\alpha = 0.01$ so that the softmax is effectively a thresholding function which outputs near binary masks. We then treat the entire concatenated parameter $\theta = [W, \Gamma]$ as trainable parameters and optimize both using ES methods. Note that this softmax method can also be seen as an instance of the continuous relaxation method from DARTS (Liu et al., 2019b). At convergence, the effective number of parameter is $ab \cdot \lambda$ where λ is the proportion of Γ' components that are non-zero. During optimization, we implement a simple heuristics that encourage sparse network: while maximizing the true environment return $f(\theta) = \sum_{t=1}^T r_t$, we also maximize the ratio $1 - \lambda$ of mask entries that are zero. The ultimate ES objective is: $f'(\theta) = \beta \cdot f(\theta) + (1 - \beta) \cdot (1 - \lambda)$, where $\beta \in [0, 1]$ is a combination coefficient which we anneal as training progresses. We also properly normalize $f(\theta)$ and $(1 - \lambda)$ before the linear combination to ensure that the procedure is not sensitive to reward scaling.

B EXTENDED BBOB EXPERIMENTAL RESULTS

B.1 CMA-ES COMPARISON

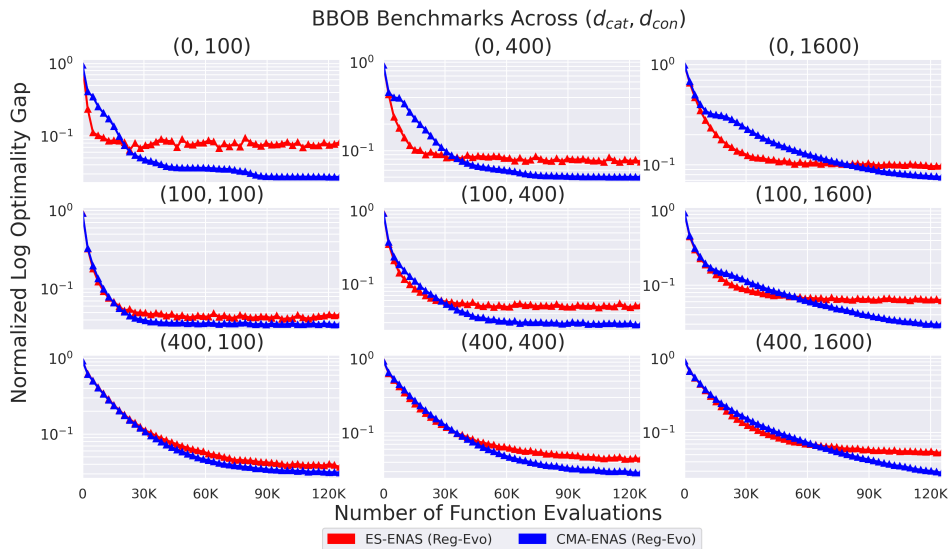


Figure 8: Comparison when regular ES/ARS is used as the continuous algorithm in ES-ENAS, vs when CMA-ES is used as the continuous algorithm (which we name “CMA-ENAS”). We use the exact same setting as Figure 2 in the main body of the paper. We use Regularized Evolution (Reg-Evo) as the default combinatorial algorithm due its strong performance found from Figure 2. We find that ES-ENAS usually converges faster initially, while CMA-ENAS achieves a better asymptotic performance. This is aligned with the results (in the first row) when comparing vanilla ES with vanilla CMA-ES. For generally faster convergence to a sufficient threshold however, ES/ES-ENAS usually suffices.

C EXTENDED NEURAL NETWORK EXPERIMENTAL RESULTS

As standard in RL, we take the mean and standard deviation of the final rewards across 3 seeds for every setting. ‘‘L’’, ‘‘H’’ and ‘‘H, H’’ stand for: linear policy, policy with one hidden layer, and policy with two such hidden layers respectively.

C.1 BASELINE METHOD COMPARISONS

In terms of the masking baseline, while (Lenc et al., 2019) fixes the sparsity of the mask, we instead initialize the sparsity at 50% and increasingly reward smaller networks (measured by the size of the mask $|m|$) during optimization to show the effect of pruning. Using this approach on several Open AI Gym tasks, we demonstrate that masking mechanism is capable of producing compact effective policies up to a high level of pruning. At the same time, we show significant decrease of performance at the 80-90% compression level, quantifying accurately its limits for RL tasks (see: Fig. 9).

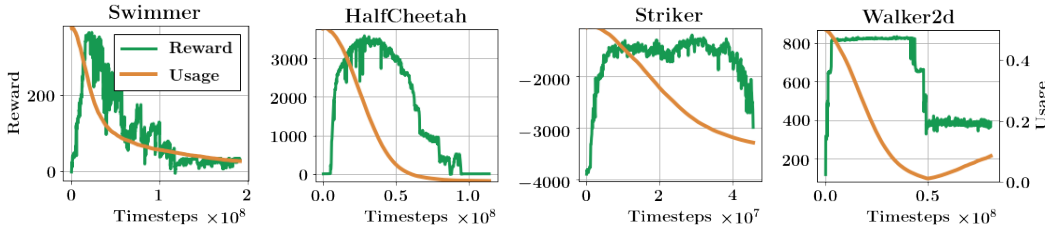


Figure 9: The results from training both a mask m and weights θ of a neural network with two hidden layers. ‘Usage’ stands for number of edges used after filtering defined by the mask. At the beginning, the mask is initialized such that $|m|$ is equal to 50% of the total number of parameters in the network.

C.2 QUANTIZATION

Env.	Dim.	Arch.	Partitions	Policy Gradient	Regularized Evolution	Random Search
Swimmer	(8,2)	L	8	366 ± 0	296 ± 31	5 ± 1
Reacher	(11,2)	L	11	-10 ± 4	-157 ± 62	-135 ± 10
Hopper	(11,3)	L	11	2097 ± 788	1650 ± 320	16 ± 0
HalfCheetah	(17,6)	L	17	2958 ± 73	3477 ± 964	129 ± 183
Walker2d	(17,6)	L	17	326 ± 86	2079 ± 1085	8 ± 0
Pusher	(23,7)	L	23	-68 ± 2	-198 ± 76	-503 ± 4
Striker	(23,7)	L	23	-247 ± 11	-376 ± 149	-590 ± 18
Thrower	(23,7)	L	23	-819 ± 8	-1555 ± 427	-12490 ± 708

Env.	Dim.	Arch.	Partitions	Policy Gradient	Regularized Evolution	Random Search
Swimmer	(8,2)	H	8	361 ± 4	362 ± 1	15 ± 0
Reacher	(11,2)	H	11	-6 ± 0	-23 ± 11	-157 ± 2
Hopper	(11,3)	H	11	3288 ± 119	2834 ± 75	95 ± 2
HalfCheetah	(17,6)	H	17	4258 ± 1034	4894 ± 110	-41 ± 5
Walker2d	(17,6)	H	17	1684 ± 1008	2026 ± 46	-5 ± 1
Pusher	(23,7)	H	23	-225 ± 131	-350 ± 236	-1049 ± 40
Striker	(23,7)	H	23	-992 ± 2	-466 ± 238	-1009 ± 1
Thrower	(23,7)	H	23	-1873 ± 690	-818 ± 363	-12847 ± 172

Table 2: Results via quantization across PG, Reg-Evo, and random search controllers. The number of partitions is always set to be $\max(|S|, |\mathcal{A}|)$.

C.3 EDGE PRUNING AND NONLINEARITY SEARCH

C.3.1 EDGE PRUNING

Env.	Dim.	Arch.	Policy Gradient	Regularized Evolution	Random Search
Swimmer	(8,2)	H	105 ± 116	343 ± 2	21 ± 1
Reacher	(11,2)	H	-16 ± 5	-52 ± 5	-160 ± 2
Hopper	(11,3)	H	3349 ± 206	2589 ± 106	66 ± 0
HalfCheetah	(17,6)	H	2372 ± 820	4016 ± 726	-156 ± 22
Walker2d	(17,6)	H	3813 ± 128	1847 ± 710	0 ± 2
Pusher	(23,7)	H	-133 ± 31	-156 ± 17	-503 ± 15
Striker	(23,7)	H	-178 ± 54	-130 ± 16	-464 ± 13
Thrower	(23,7)	H	-532 ± 29	-1107 ± 158	-7797 ± 112

Table 3: Results via quantization across PG, Reg-Evo, and random search controllers. The number of edges is always set to be 64 in total, or (32, 32) across the two weight matrices when using a single hidden layer.

C.3.2 NONLINEARITY SEARCH

Intriguingly, we found that appending the extra nonlinearity selection into the edge-pruning search space improved performance across HalfCheetah and Swimmer, but not across all environments (Fig). However, lack of total improvement is consistent with the results found with WANNs (Gaier & Ha, 2019), which also showed that trained WANNs’ performances matched with vanilla policies. From these two observations, we hypothesize that perhaps nonlinearity choice for simple MLP policies trained via ES are not quite so important to performance as other components, but more ablation studies must be conducted. Furthermore, for quantization policies, we see that hidden layer policies near-universally outperform linear policies, even when using the same number of distinct weights.

Env.	Dim.	Arch.	Policy Gradient	Regularized Evolution	Random Search
Swimmer	(8,2)	H	247 ± 110	359 ± 5	11 ± 3
Hopper	(11,3)	H	2270 ± 1464	2834 ± 120	57 ± 7
HalfCheetah	(17,6)	H	3028 ± 469	5436 ± 978	-268 ± 29
Walker2d	(17,6)	H	1057 ± 413	2006 ± 248	0 ± 1

Table 4: Results using the same setup as Table 3, but allowing nonlinearity search.

Env.	Dim.	(PG, Reg-Evo) Reward	Method
HalfCheetah	(17,6)	(2958, 3477) → (4258, 4894)	Quantization (L → H)
Hopper	(11,3)	(2097, 1650) → (3288, 2834)	Quantization (L → H)
HalfCheetah	(17,6)	(2372, 4016) → (3028, 5436)	Edge Pruning (H) → (+ Nonlinearity Search)
Swimmer	(8,2)	(105, 343) → (247, 359)	Edge Pruning (H) → (+ Nonlinearity Search)

Table 5: Rewards for selected environments and methods, each result averaged over 3 seeds. Arrow denotes modification or addition (+).

D NETWORK VISUALIZATIONS

D.1 QUANTIZATION

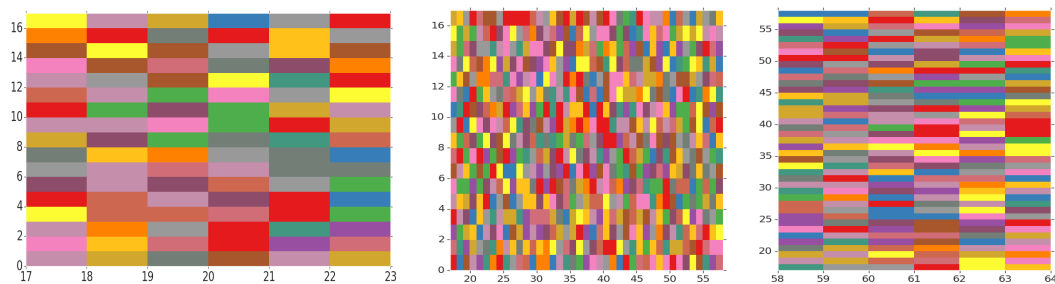


Figure 10: (a): Partitioning of edges into distinct weight classes obtained for the linear policy for HalfCheetah environment from OpenAI Gym. (b): Partitioning of edges for a policy with one hidden layer encoded by two matrices. State and action dimensionalities are: $s = 17$ and $a = 6$ respectively and hidden layer for the architecture from (b) is of size 41. Thus the size of the matrices are: 17×6 for the linear policy from (a) and: 17×41 , 41×6 for the nonlinear one from (b).

D.2 EDGE PRUNING

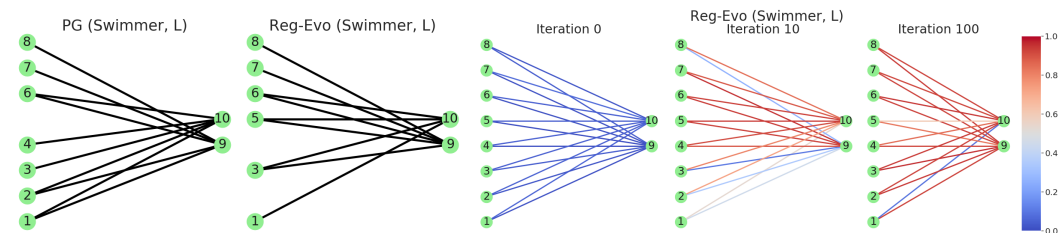


Figure 11: (Left): Final architectures that PG and Reg-Evo converged to on Swimmer with a linear (L) policy, as specified in Subsection 3.3.3. Note that the controller does not select all edges even if it is allowed in the boolean search space, but also *ignores some state values*. (Right): Convergence result for Reg-Evo, similar to Fig. 6 in Subsection 3.3.3.